Electronic Supplementary Material (ESI) for Dalton Transactions.

Solvent-free synthesis of new inorganic-organic hybrid solids with finely tuned manganese oxalate structures

Lindong Luan,[a] Jing Li,[b] Changzhen Yin,[b] Zhien Lin,*[b] and Hui Huang*[a]

[a] *School of Chemistry, Beijing Institute of Technology, Beijing 100081, P. R. China.*

[b] *College of Chemistry, Sichuan University, Chengdu 610064, P. R. China.*

* To whom correspondence should be addressed. Tel: +86-28-85412284. E-mail: zhienlin@scu.edu.cn; huanghui@caep.ac.cn

Physical measurements:

IR spectra (KBr pellets) were recorded on a Nicolet Impact 410 FTIR spectrometer. Powder X-ray diffraction (XRD) data were obtained using a Rigaku D/MAX-rA diffractometer with Cu-Kα radiation (λ = 1.5418 Å). The thermogravimetric analyses were performed on a Netzsch STA 449c analyzer in a flow of N_2 with a heating rate of 10 ºC/min. Magnetic measurements were performed at 5 kG in the temperature range 2-300 K with a SQUID MPMS-7 magnetometer manufactured by Quantum Design. Background corrections for the sample holder assembly and diamagnetic components of the compound were applied. Single crystal X-ray diffraction data were collected on a New Gemini, Dual, Cu at zero, EosS2 diffractometer with Cu Kα (λ = 1.54184 Å) at room temperature. The crystal structures were solved by direct methods. The structures were refined on F^2 by full-matrix least-squares methods using the *SHELXTL* program package.[1]

Reference

1. G. M. Sheldrick, Acta Cryst., Sect. A, 2008, 64, 112.

Synthesis

Synthesis of $(H_2mpip)_{1.5}{\cdot}Mn_3(HPO_4)(H_2PO_4)(ox)_3$ (1): A mixture of MnO (0.213 g), $H_2C_2O_4{\cdot}2H_2O$ (0.378 g), H_3PO_4 (85 wt%, 135 μL), and 1-methylpiperazine (165 μL) was sealed in a Teflon-lined stainless steel autoclave and heated at 150 °C for 8 d. The autoclave was subsequently allowed to cool to room temperature. Yellow crystals were recovered by filtration, washed with distilled water, and finally dried at ambient temperature (81 % yield based on manganese).

Synthesis of $H_2dap{\cdot}Mn_2(HPO_4)(ox)_2$ (2): A mixture of MnO (0.142 g), $H_2C_2O_4{\cdot}2H_2O$ (0.252 g), H_3PO_4 (85 wt%, 135 μL), and 1,2-diaminopropane (85 μL) was sealed in a Teflon-lined stainless steel autoclave and heated at 150 °C for 7 d. The autoclave was subsequently allowed to cool to room temperature. Yellow crystals were recovered by filtration, washed with distilled water, and finally dried at ambient temperature (41 % yield based on manganese).

Synthesis of $Hpa{\cdot}Mn_2(H_2PO_4)(ox)_2$ (3): A mixture of MnO (0.142 g), $H_2C_2O_4{\cdot}2H_2O$ (0.252 g), H_3PO_4 (85 wt%, 135 μL), and propylamine (165 μL) was sealed in a Teflon-lined stainless steel autoclave and heated at 150 °C for 8 d. The autoclave was subsequently allowed to cool to room temperature. Yellow crystals were recovered by filtration, washed with distilled water, and finally dried at ambient temperature (75 % yield based on manganese).

Table 1. CHN elemental analysis results

	anal. found	calc
compound **1**	C 20.55%, H 3.03%, N 5.46%	C 20.92%, H 3.12%, N 5.42%
compound **2**	C 18.07%, H 2.78%, N 6.05 %	C 18.36%, H 2.86%, N 6.12 %
compound **3**	C 18.92%, H 2.68%, N 3.04%	C 18.98%, H 2.73%, N 3.16 %

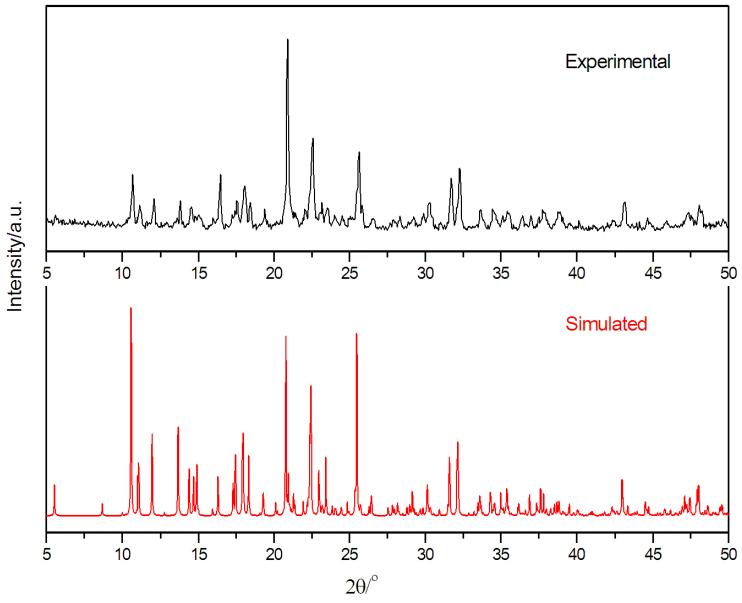

Fig. S1. Experimental and simulated powder XRD patterns of compound **1**.

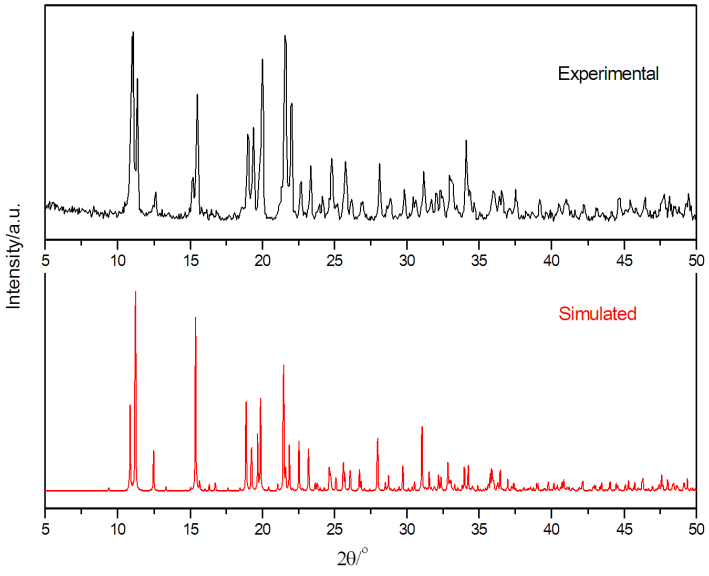

Fig. S2. Experimental and simulated powder XRD patterns of compound **2**.

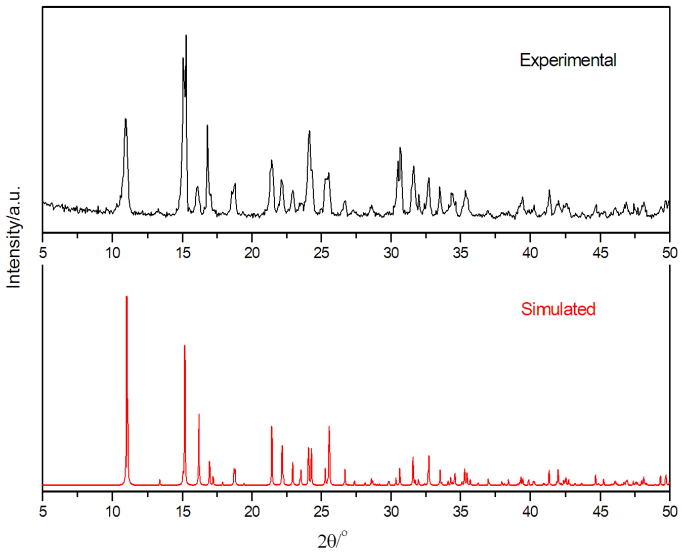

Fig. S3. Experimental and simulated powder XRD patterns of compound **3**.

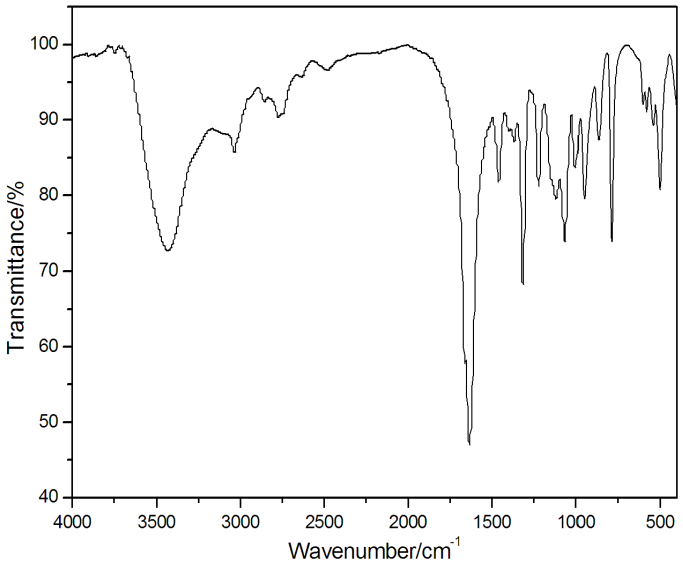

Fig. S4. IR spectrum of compound **1**.

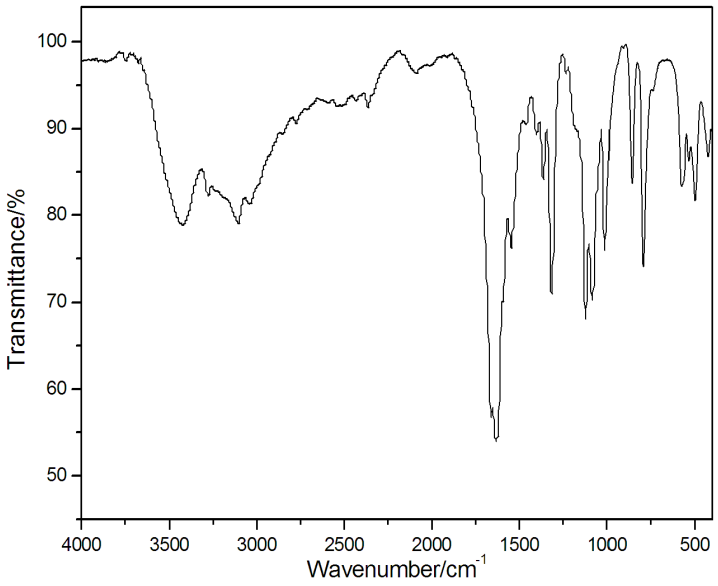

Fig. S5. IR spectrum of compound **2**.

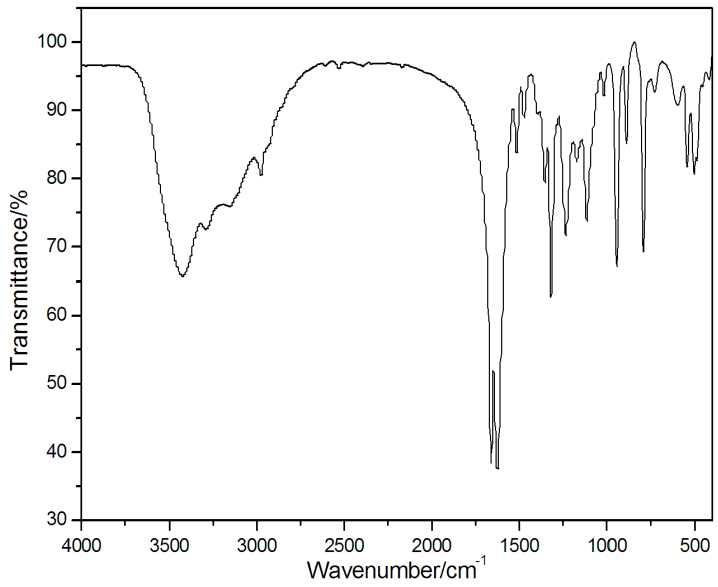

Fig. S6. IR spectrum of compound **3**.

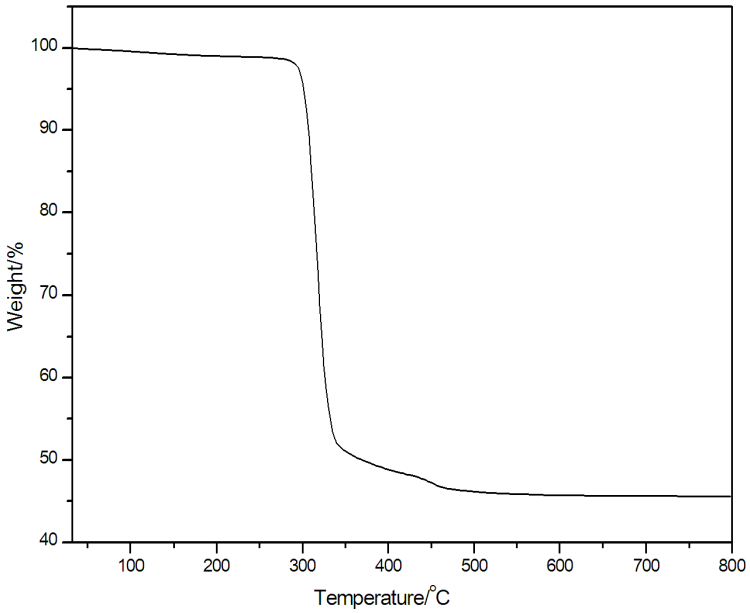

Fig. S7. TGA curve of compound **1**.

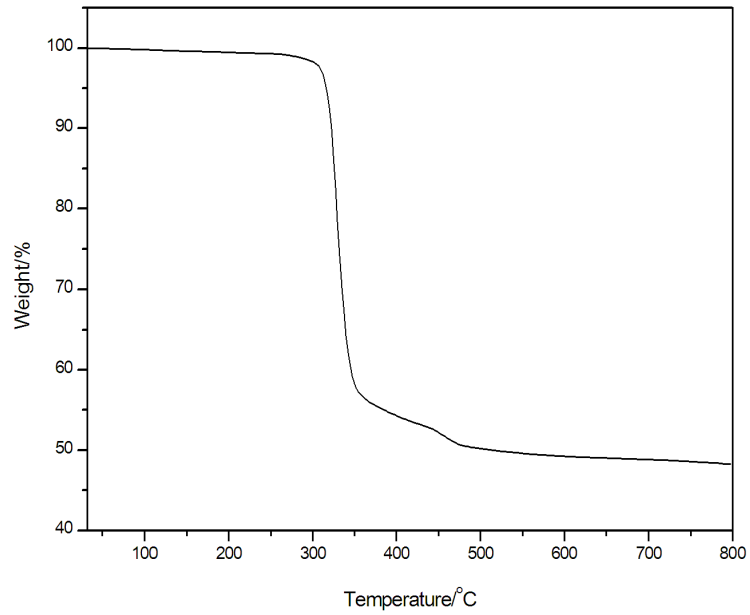

Fig. S8. TGA curve of compound **2**.

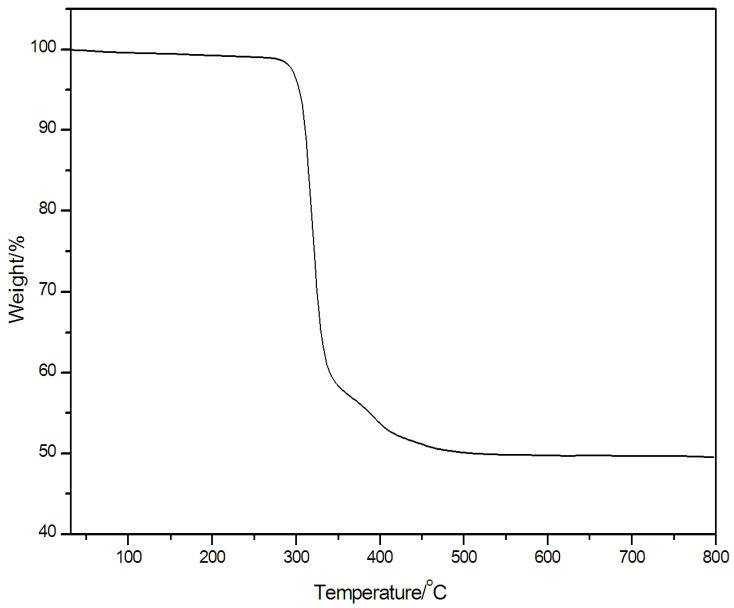

Fig. S9. TGA curve of compound **3**.

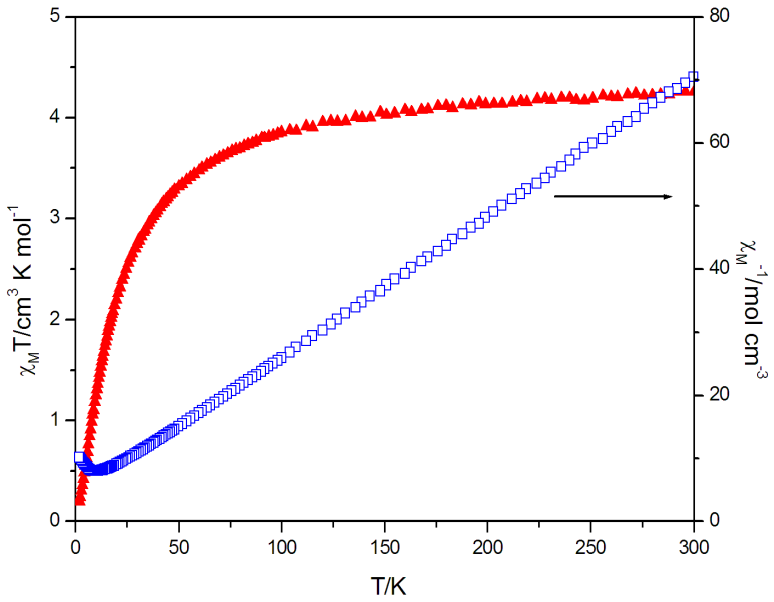

Fig. S10. Temperature dependence of $\chi_M T$ and χ_M^{-1} for compound **1**.

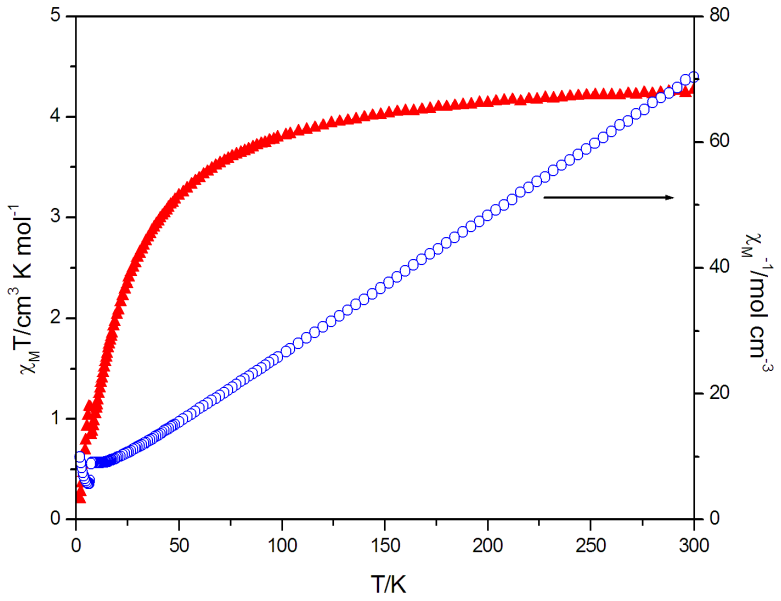

Fig. S11. Temperature dependence of $\chi_M T$ and χ_M^{-1} for compound **2**.

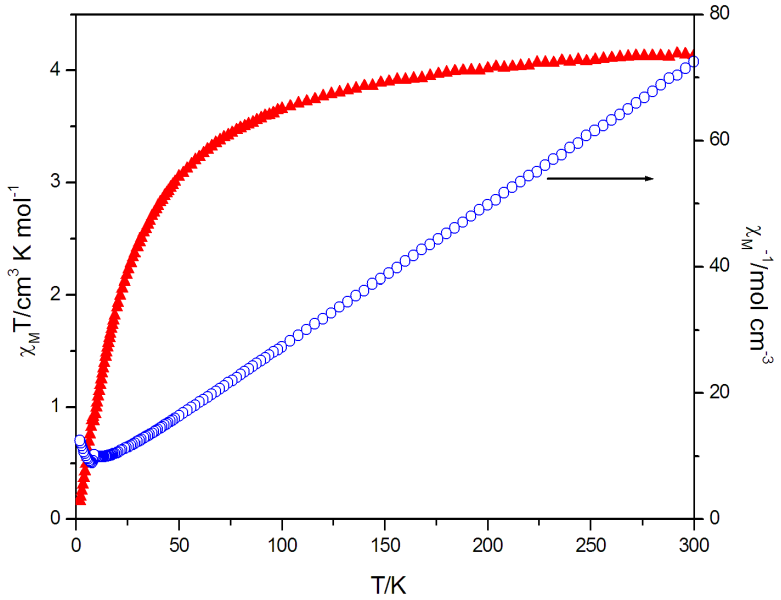

Fig. S12. Temperature dependence of $\chi_M T$ and χ_M^{-1} for compound **3**.

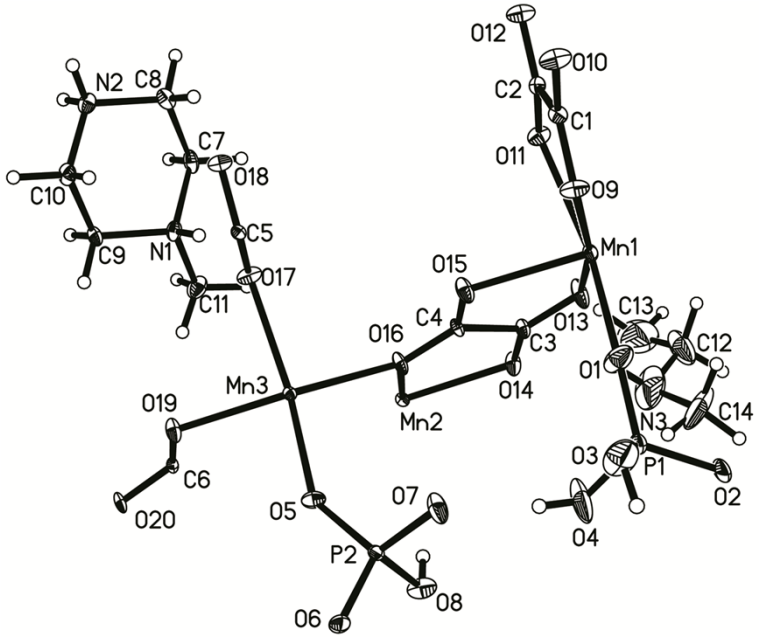

Fig. S13. ORTEP plot of the asymmetric unit of compound **1**, showing the labeling scheme and the 30% probability displacement ellipsoid.

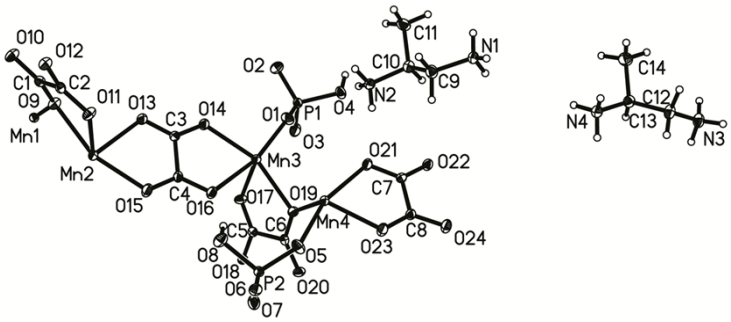

Fig. S14. ORTEP plot of the asymmetric unit of compound **2**, showing the labeling scheme and the 30% probability displacement ellipsoid.

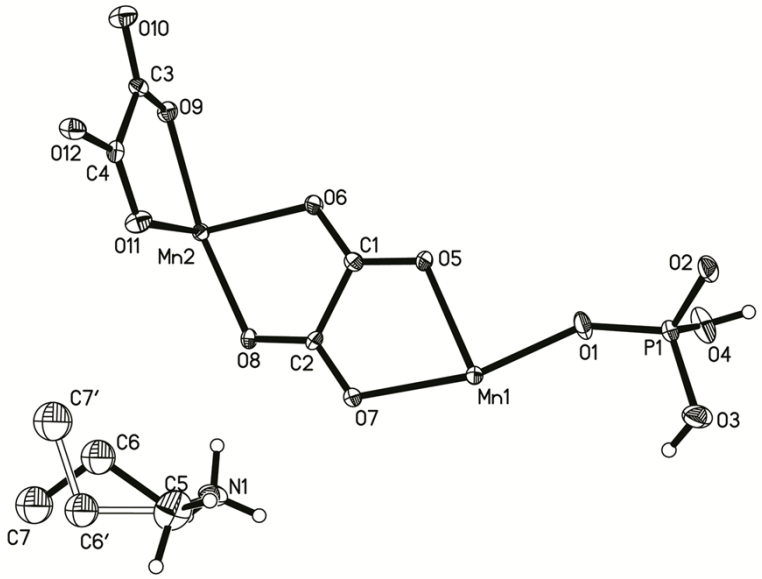

Fig. S15. ORTEP plot of the asymmetric unit of compound **3**, showing the labeling scheme and the 30% probability displacement ellipsoid.

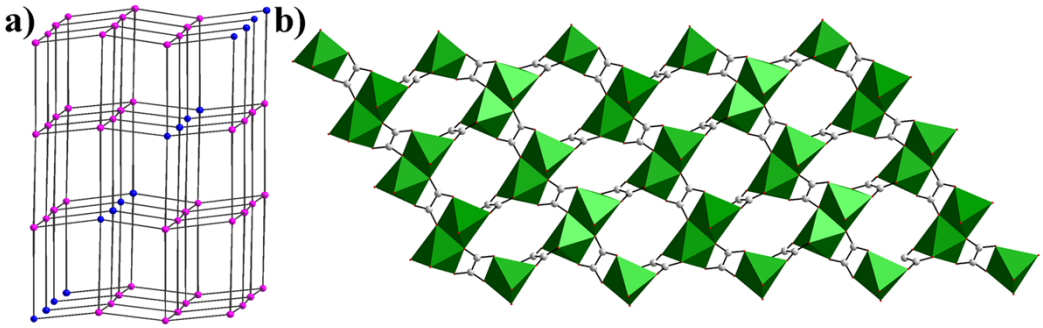

Fig. S16. (Left) A hypothetical interrupted pcu-topology with the Mn_2O_{10} to Mn_2P_2 ratio of 3:1. Purple ball: Mn_2O_{10} dimer; blue ball: Mn_2P_2 tetramer. (Right) This compound possesses a new $Mn_8(ox)_8$ nanobelt with the width of ca. 17.5 Å.